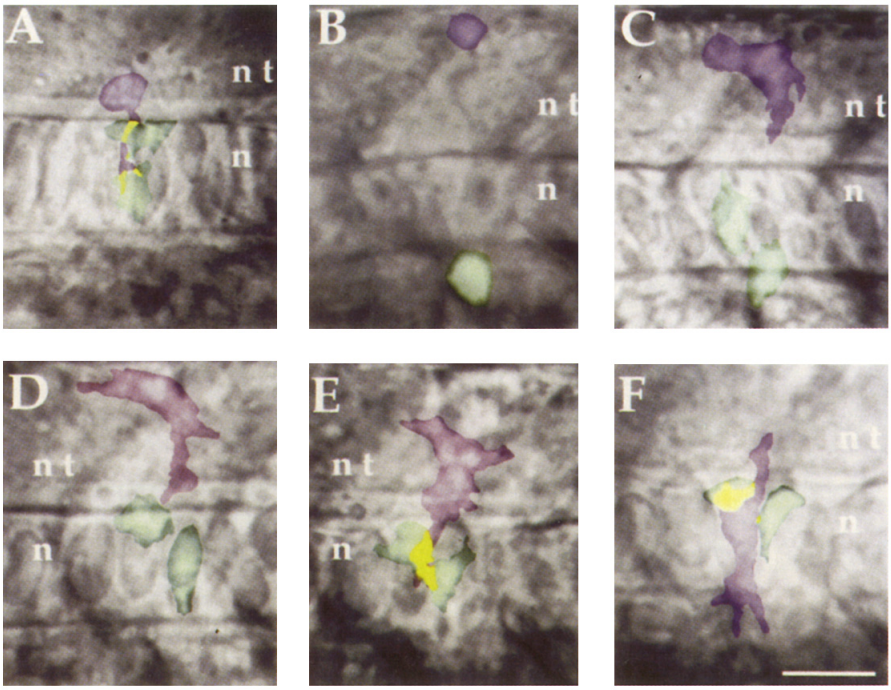

Figure 2.5 In zebrafish, anterior sclerotome cells share a migration pathway with motor axons and neural crest cells. Individual sclerotome cells were labeled green by injection of fluorescein dextran and individual motor neurons and neural crest cells were labeled magenta by injection of rhodamine dextran; yellow indicates regions of overlap within a single focal plane. (A) Overlap between the ventrally extending axon of an identified motor neuron, CaP, and a dorsally migrating anterior sclerotome cell. (B–F) Time series of a single, ventrally migrating neural crest cell and a single dorsally migrating sclerotome cell followed over 6 hours in a living embryo. The sclerotome cell divided once during this time. n, notochord; nt, neural tube. Bar = 21 μm. (Reproduced, with permission of Company of Biologists Ltd, from Morin-Kensicki and Eisen, 1997.)

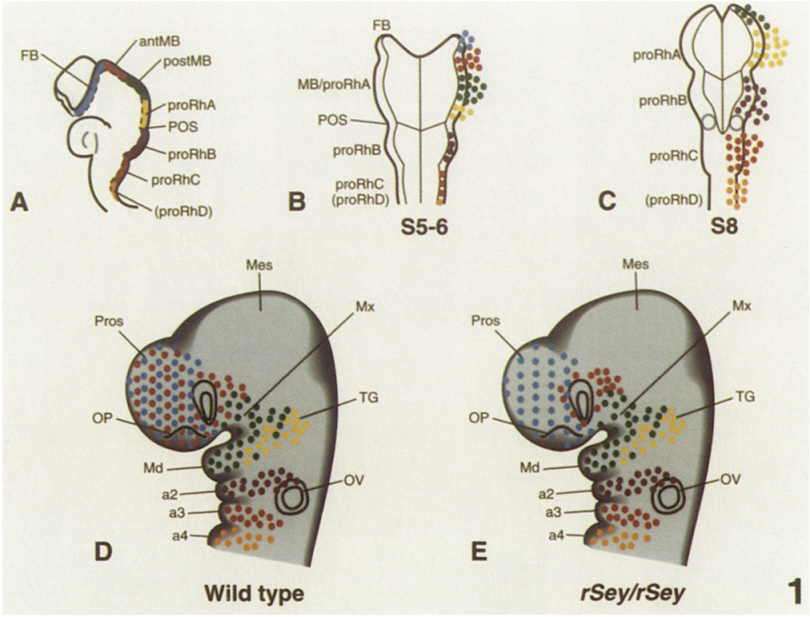
FB
antMB
postMB
proRhA
POS
proRhB
proRhC
(proRhD)
A
FB
MB/proRhA
POS
proRhB
proRhC
(proRhD)
B
S5-6
proRhA
proRhB
proRhC
(proRhD)
C
S8
Mes
Pros
Mx
TG
OP
Md
OV
a2
a3
a4
D
Wild type
Mes
Pros
Mx
TG
OP
Md
OV
a2
a3
a4
E
rSey/rSey
1

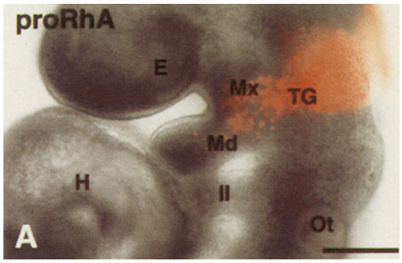
proRhA
E
Mx
TG
Md
H
II
Ot
A

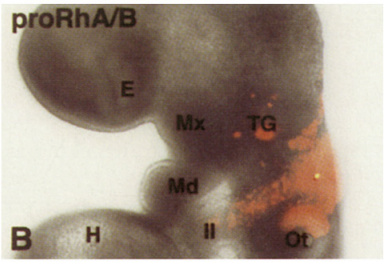
proRhA/B
E
Mx
TG
Md
B
H
II
Ot

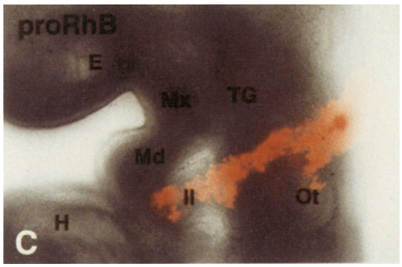
proRhB
E
Mx
TG
Md
II
Ot
H
C

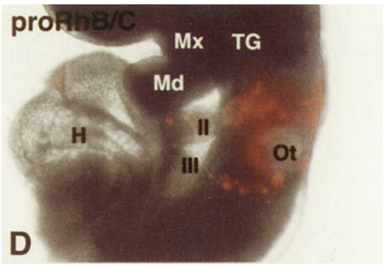
proRhB/C
Mx
TG
Md
H
II
III
Ot
D

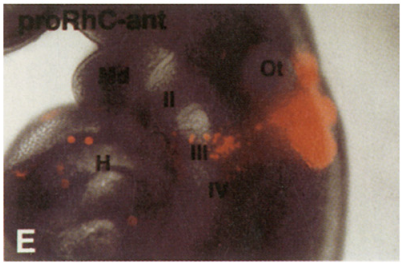
proRhC-ant
Md
Ot
II
H
III
IV
E

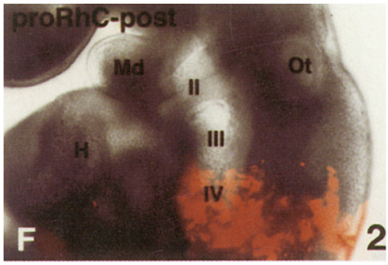
proRhC-post
Md
Ot
II
H
III
IV
F
2

Figure 3.7 Panel 1: Diagrams showing migration patterns of cranial crest cells in mouse and rat embryos. (A, B) Lateral and dorsal views at 5–6ss. (C) Dorsal view at 8ss. (D, E) Lateral view of wild-type and homozygous *rSey* embryos, respectively, at the pharyngula stage. (A) At the time of mammalian cranial crest cell emigration, four morphological units are present in the rostral neural plate, from anterior to posterior: forebrain (FB); midbrain (MB, anterior MB, posterior MB) + presumptive prorhombomere A (proRhA, rostral hindbrain); proRhB (preotic hindbrain); and proRhC + presumptive proRhD (caudal hindbrain); preotic sulcus (POS) is an obvious landmark in the hindbrain. Regions in which DiI labeling of crest cells was performed are shown by different colors. (B) Unlike crest cells in other animals and trunk crest cells, cranial crest cells in mammals emigrate from the neuroepithelium before its closure. At 5–6ss, crest cells begin emigrating from the forebrain and midbrain/proRhA region. (C) At 8ss, zones free of crest cells exist at the boundaries between proRhA/B (preotic sulcus) and proRhB/C, thereby making three streams in the hindbrain region. The forebrain cannot be seen in this view. (D) Normal embryo at the developmental stage in which migration of cranial crest cells is nearly complete. The most anteriorly situated facial primordium is the frontonasal prominence underlying the olfactory placode (OP), to which crest cells from both the forebrain and midbrain migrate. Caudally, the first pharyngeal (branchial) arch appears, later developing into the maxillary (Mx) and mandibular (Md) prominences which are, respectively, the primordia of upper and lower jaws. Situated further caudally are the second, third, and fourth pharyngeal arches (a2, a3, and a4). Crest cells derived from the posterior midbrain and proRhA migrate to the first arch, those from the proRhB to the second arch, and those from proRhC and proRhD to the third and fourth arches, respectively. (E) In homozygous *rSey* embryos, migration of midbrain crest cells into the frontonasal region is specifically impaired, though crest cells from other regions migrate normally. OV, otic vesicle; TG, trigeminal ganglion. (Reproduced, with permission, from Osumi-Yamashita *et al.*, 1997.) Panel 2: Segmental distribution of neural crest cells labeled at proRhA (A), proRhB (C), anterior region of proRhC (E), and posterior region of proRhC (F), as well as at the boundaries between proRhA and proRhB (B), and between proRhB and proRhC (D). Synthesized images of bright-field and corresponding dark-field images of lateral views of whole-mount embryos. Mx, maxillary prominence; TG, trigeminal ganglion; Ot, otic vesicle; II, second pharyngeal arch; III, third pharyngeal arch; IV, fourth pharyngeal arch; H, heart primordium. Bar = 200 μm. (Reproduced, with permission, from Osumi-Yamashita *et al.*, 1996.)

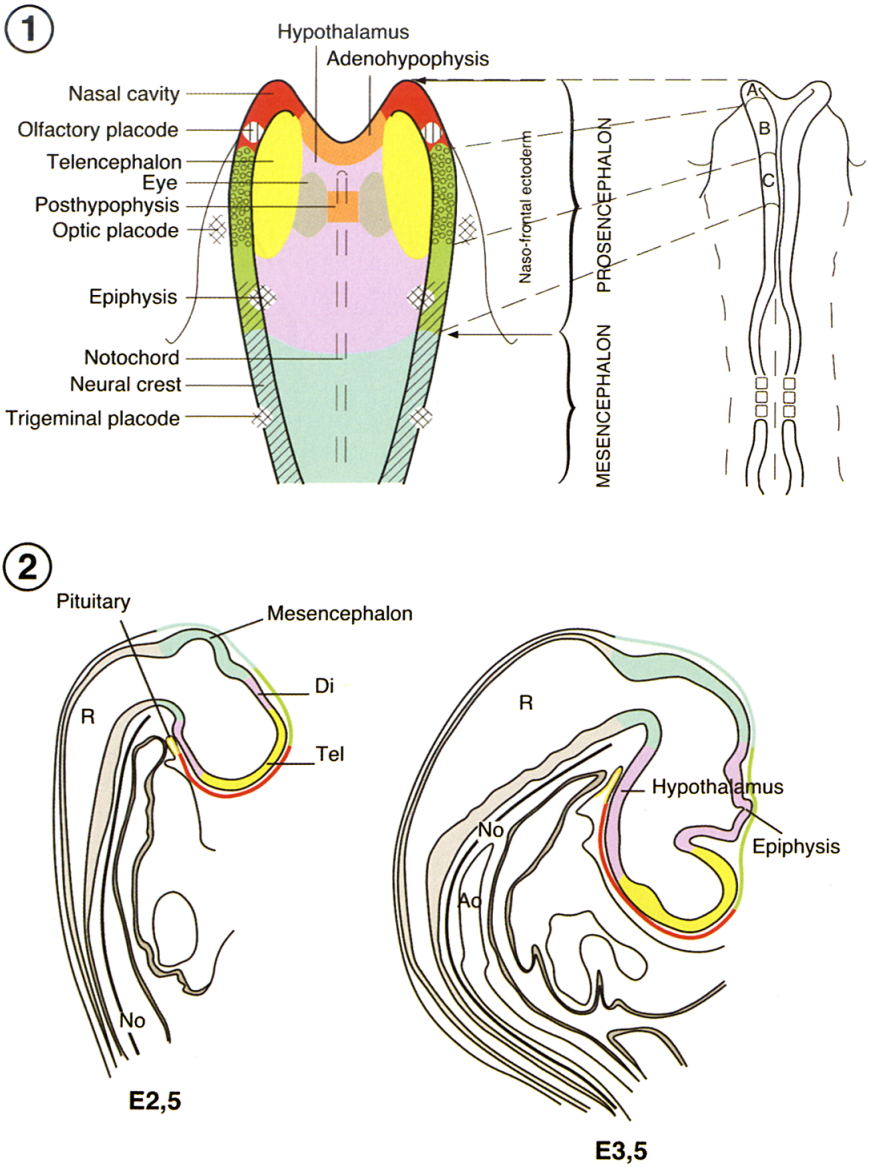

Figure 3.8 Fate map of the neural plate in an avian embryo at 3ss. (1) The neural plate is represented flat with its limiting anterior and lateral neural folds. This map was deduced from substitution experiments of fragments of the neural fold as drawn in the embryo represented on the right. Other experiments involved grafting of the anterior neural fold which yields Rathke's pouch and of definite regions of the neural plate (see Couly and Le Douarin, 1987, for details). (2) Diagram showing the evolution of the territories represented on the fate map in (1). It appears that the two territories corresponding to the telencephalon join on the dorsal midline and extend more rostrally than the level of the hypothalamus and of Rathke's pouch (which yields the adenohypophysis). That part of the brain which develops rostrally to the tip of the notochord (No) is later covered by neural crest-derived bones. Ao, dorsal aorta; R, rhombencephalon; Di, diencephalon; Tel, telencephalon.

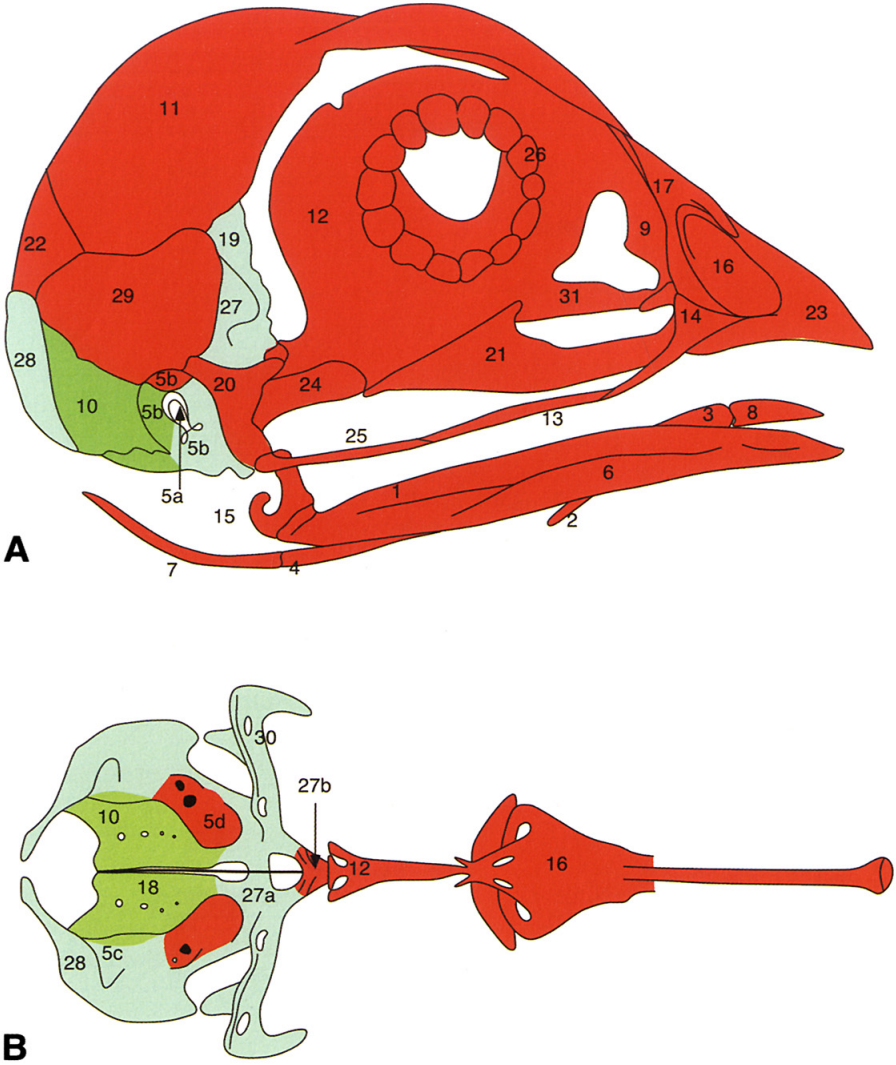

Figure 3.9 Contribution of the neural crest (red), the cephalic mesenchyme (blue), and the somitic mesoderm (green) to the vertebrate cranium. (A) Lateral view of the cephalic skeleton of a 14-day-old avian embryo. (B) Basal view of the chondrocranium of a 10-day-old embryo. 1, angular; 2, basibranchial; 3, basihyal; 4, ceratobranchial; 5a, columella; 5b, otic capsule; 5c, otic capsule (pars ampullaris); 5d, otic capsule (pars cochlearis); 6, dentary; 7, epibranchial; 8, entoglossum; 9, ethmoid; 10, exoccipital; 11, frontal; 12, interorbital septum; 13, jugal; 14, maxilla; 15, Meckel's cartilage; 16, nasal capsule; 17, nasal; 18, basioccipital; 19, postoccipital; 20, quadrate; 21, palatine; 22, parietal; 23, premaxilla; 24, pterygoid; 25, quadratojugal; 26, scleral ossicles; 27a, basipostsphenoid; 27b, basipresphenoid; 28, supraoccipital; 29, squamosal; 30, orbital capsule; 31, vomer. (Reproduced, with permission of Company of Biologists Ltd, from Couly *et al.*, 1993.)

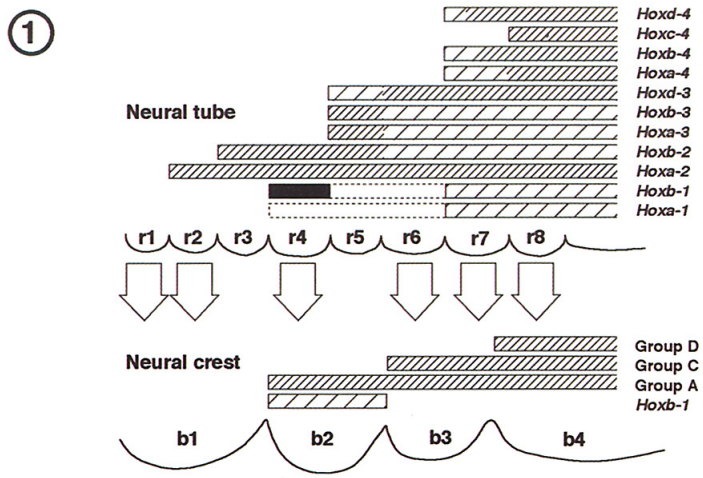
1
Neural tube
Hoxd-4
Hoxc-4
Hoxb-4
Hoxa-4
Hoxd-3
Hoxb-3
Hoxa-3
Hoxb-2
Hoxa-2
Hoxb-1
Hoxa-1
r1
r2
r3
r4
r5
r6
r7
r8
Neural crest
Group D
Group C
Group A
Hoxb-1
b1
b2
b3
b4

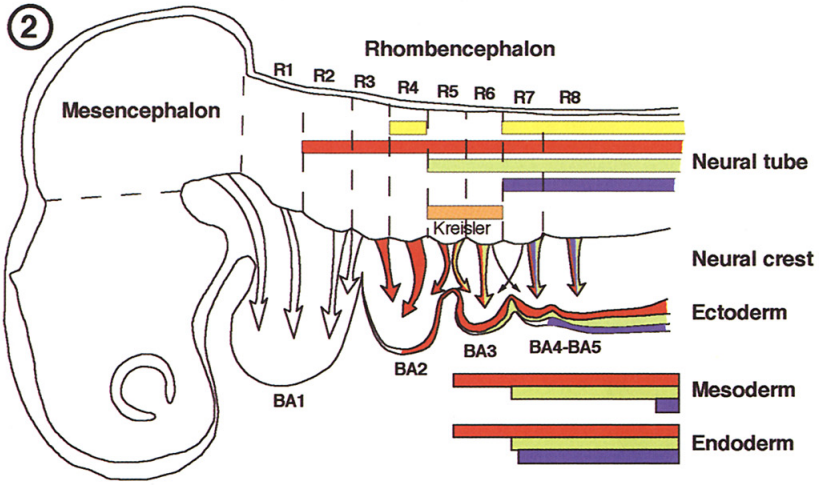
2
Rhombencephalon
R1
R2
R3
R4
R5
R6
R7
R8
Mesencephalon
Neural tube
Kreisler
Neural crest
Ectoderm
BA1
BA2
BA3
BA4-BA5
Mesoderm
Endoderm

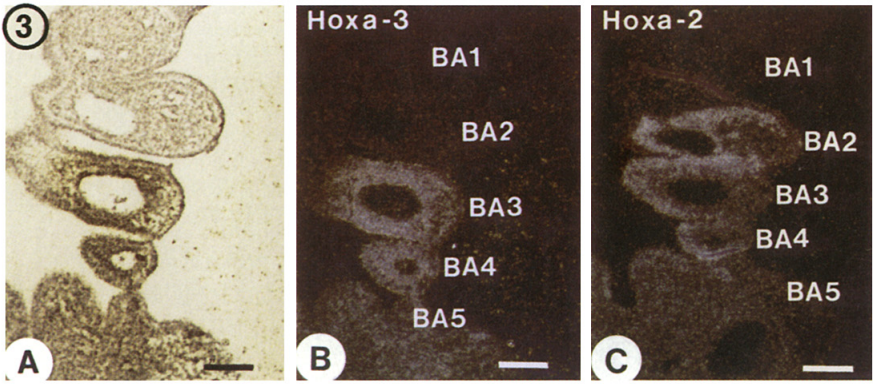
3
A
Hoxa-3
BA1
BA2
BA3
BA4
BA5
B
Hoxa-2
BA1
BA2
BA3
BA4
BA5
C

Figure 3.16 Summary of *Hox* gene expression in the hindbrain and corresponding neural crest cells. Panel 1: Filled area denotes region of upregulated *Hoxb-1* expression. Dense hatching denotes areas of high-level expression, sparse hatching denotes areas of lower-level expression. Dotted lines show transient gene expression; b1–b4, branchial arches. (Reproduced, with permission of Company of Biologists Ltd, from Prince and Lumsden, 1994.) Panel 2: Schematic representation of the expression of certain *Hox* genes of the first paralogous groups in chick or quail embryos at E3 when the branchial arches (BA) are being colonized by neural crest cells originating from the posterior half of the mesencephalon and the rhombomeres (R1–R8). The arrows indicate the anteroposterior origin of the neural crest cells migrating to each BA. Expression of *Hox* genes is also indicated in the superficial ectoderm. Panel 3: Frontal sections of a chick embryo at E3 showing *Hoxa-3* (A, B) and *Hoxa-2* (C). *In situ* hybridization with the *Hoxa-3* probe seen in bright-field illumination (A). (B, C) Dark-field pictures of *Hoxa-3* (B) and *Hoxa-2* (C). Bar = 100 μm. (Reproduced, with permission of Company of Biologists Ltd, from Couly *et al.*, 1996.)

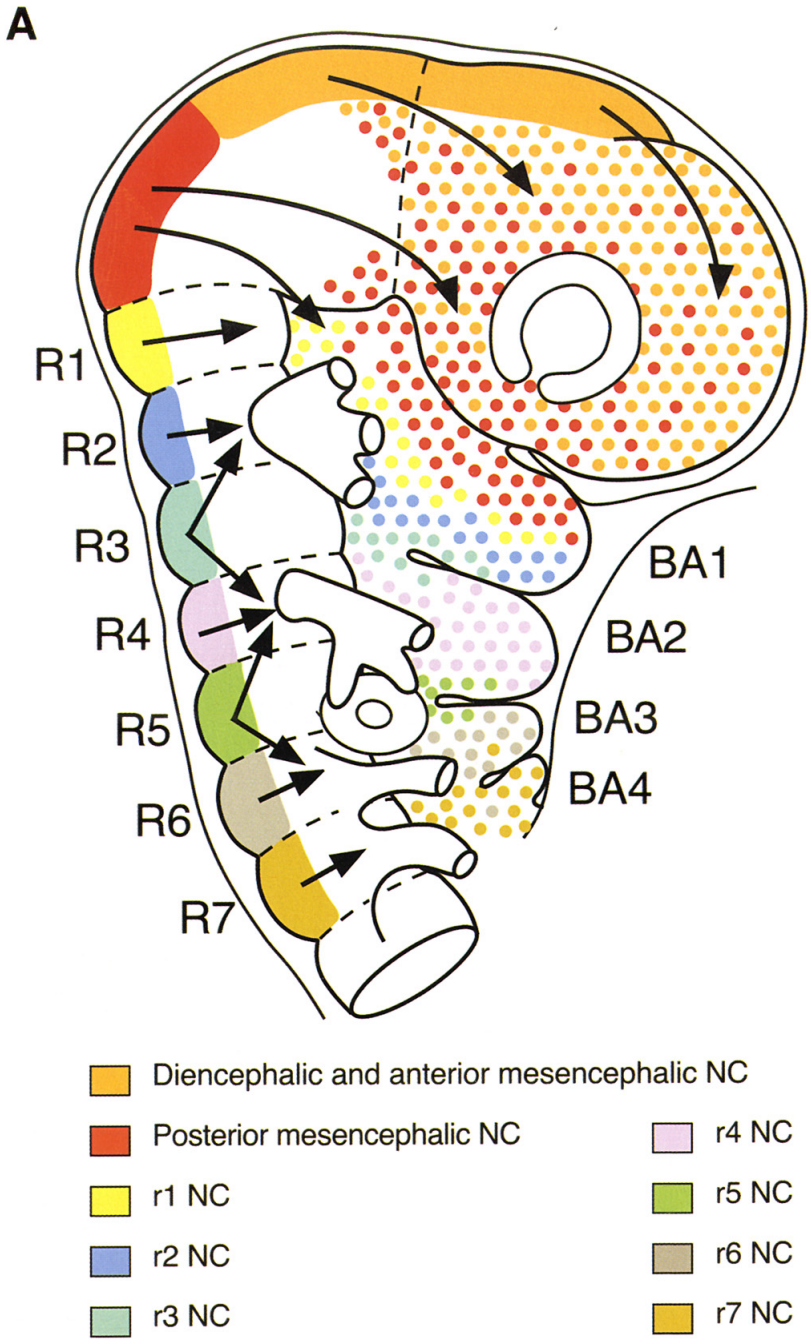
A
R1
R2
R3
R4
R5
R6
R7
BA1
BA2
BA3
BA4
Diencephalic and anterior mesencephalic NC
Posterior mesencephalic NC
r1 NC
r2 NC
r3 NC
r4 NC
r5 NC
r6 NC
r7 NC

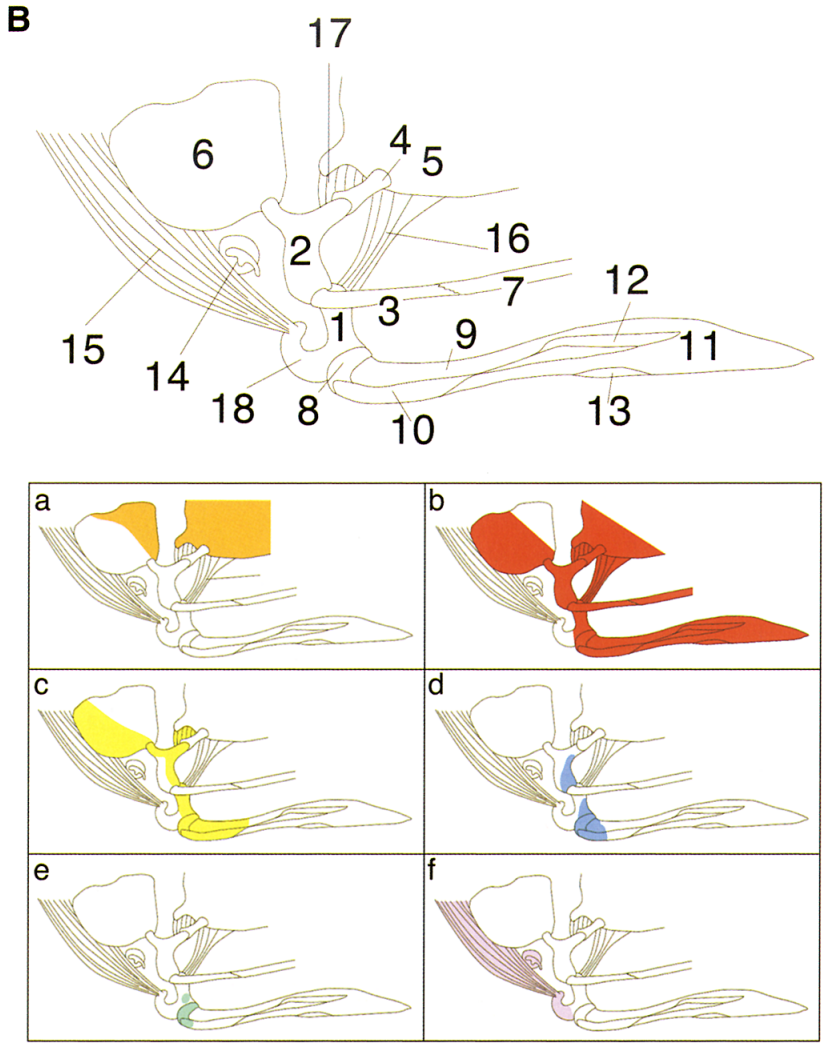

Figure 3.20 (A) Migration map of cephalic neural crest cells in the avian embryo. The origin of neural crest cells found in the nasofrontal and periocular mass and in the branchial arches is color-coded. Anterior mesencephalon contributes to the nasofrontal and periocular mass. Posterior mesencephalon also participates in these structures, but in addition populates the anterodistal part of BA1. The complementary portion of BA1 derives from R1/R2 together with a small contribution of R3. The major contribution to BA2 comes from R4. Neural crest cells arising from R3 and R5 split into strains participating, respectively, to two adjacent arches: R3 cells migrate to BA1 and BA2; R5 cells migrate to BA2 and BA3. R6 and R7 derived cells migrate to BA3 and BA4. (B) Color-coded (see A) fate map of the neural crest issued from the prosencephalon, mesencephalon, and rhombomeres 1–4. The bones, cartilages, and muscles of the jaw are numbered in the upper panel. 1, articular; 2, quadrate; 3, quadratojugal; 4, pterygoid; 5, palatine; 6, squamosal; 7, jugal; 8, Meckel's cartilage; 9, supra-angular; 10, angular; 11, dentary; 12, opercular; 13, splenial; 14, columella; 15, depressor mandibulae; 16, pterygoideus; 17, pterygoquadrate; 18, retroarticular process.

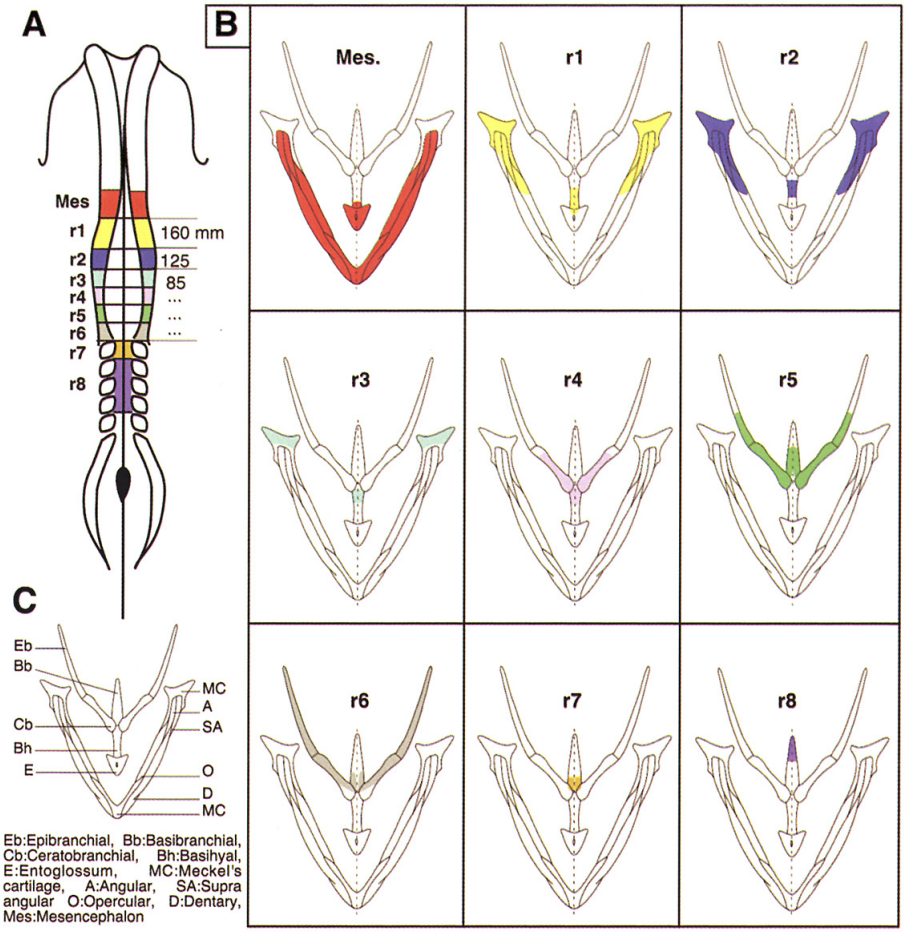

Figure 3.21 Respective origins of the lower jaw and hyoid bone from midbrain and hindbrain neural crest. (A, B) Results of experiment whereby the chick neural folds corresponding to each individual rhombomere and to the posterior mesencephalic half, were substituted by their quail counterpart at 5ss. (C) Lower jaw and hyoid bones with the corresponding legends. (Reproduced, with permission of Company of Biologists Ltd, from Couly *et al.*, 1996.)

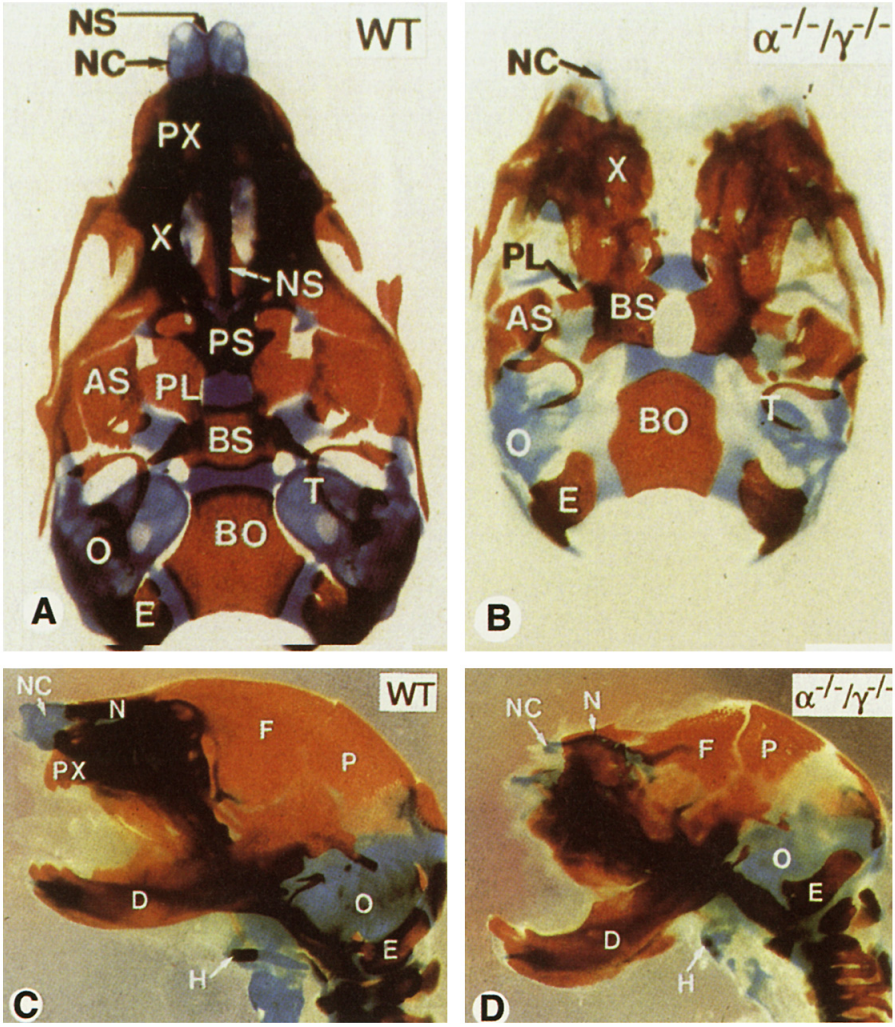

Figure 3.29 Craniofacial skeletal features of 18.5 dpc wild-type (WT) and RAR double $\alpha^{-/-}/\gamma^{-/-}$ mutant fetuses. Comparison of ventral (A, B) and lateral (C, D) views of the skull and of the dentary bone between wild-type (A, C) and RAR$\alpha^{-/-}/\gamma^{-/-}$ mutant (B, D) fetuses. In the mutant, note the nearly complete absence of the nasal capsule (NC), the complete agenesis of the nasal septum (NS) and of the premaxillary (PX) and presphenoid (PS) bones, the wide median cleft in the basisphenoid bone (BS), and the aplasia of the hyoid bone (H). AS, alisphenoid bone; BO, basioccipital bone; BS, basisphenoid bone; D, mandibular (dentary) bone; E, exoccipital bone; F, frontal bone; N, nasal bone; NC, nasal capsule; NS, nasal septum; O, otic capsule; P, parietal bone; PL, palatine bone; PS, presphenoid bone; PX, incisive (premaxillary) bone; T, tympanic bone; X, maxillary bone. (Reproduced, with permission of Company of Biologists Ltd, from Lohnes *et al.*, 1995.)

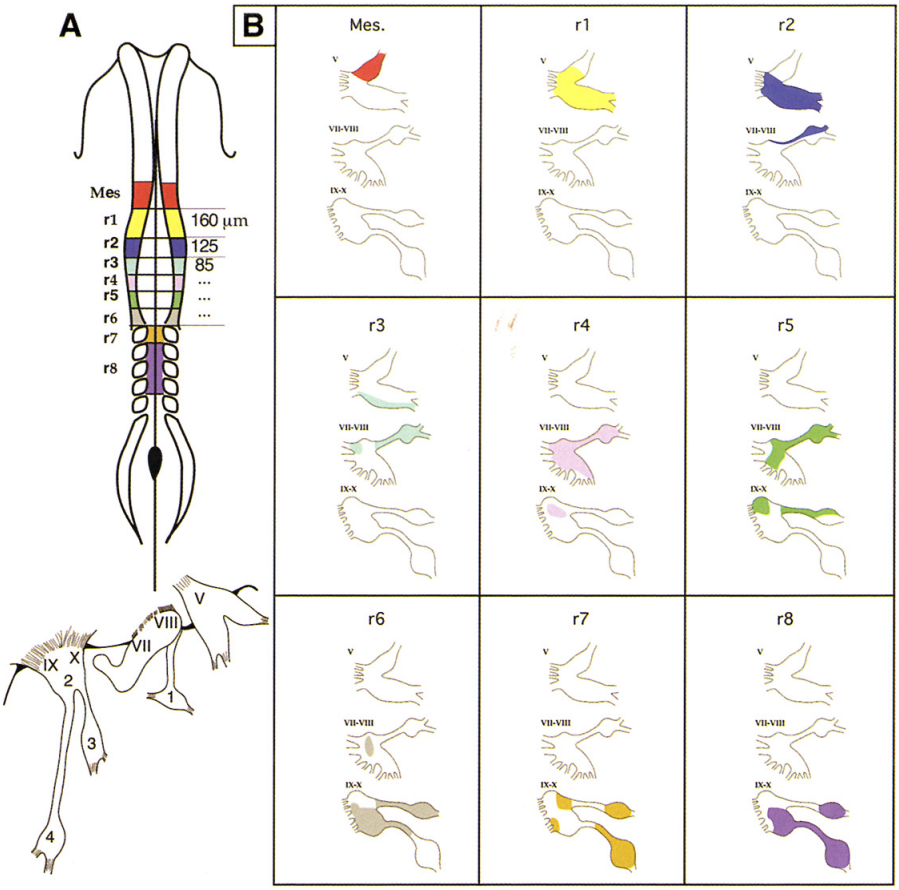

Figure 4.6 The contribution of mesencephalic- and rhombencephalic-level neural crest to the formation of cranial sensory ganglia. Isotopic and isochronic grafts of quail neural primordium into chick hosts at 5ss. (A) Color-coded scheme illustrating the different transplanted regions. (B) Colonization patterns of different portions of the cranial ganglia by the grafted fragments of neural primordia. Mes, mesencephalon; r, rhombomere; V, trigeminal ganglion; VII, facial ganglion; VIII, vestibuloacoustic ganglion; IX, glossopharyngeal ganglion; X, vagal ganglion; 1, geniculate ganglion; 2, superior jugular ganglion; 3, petrosal ganglion; 4, nodose ganglion.

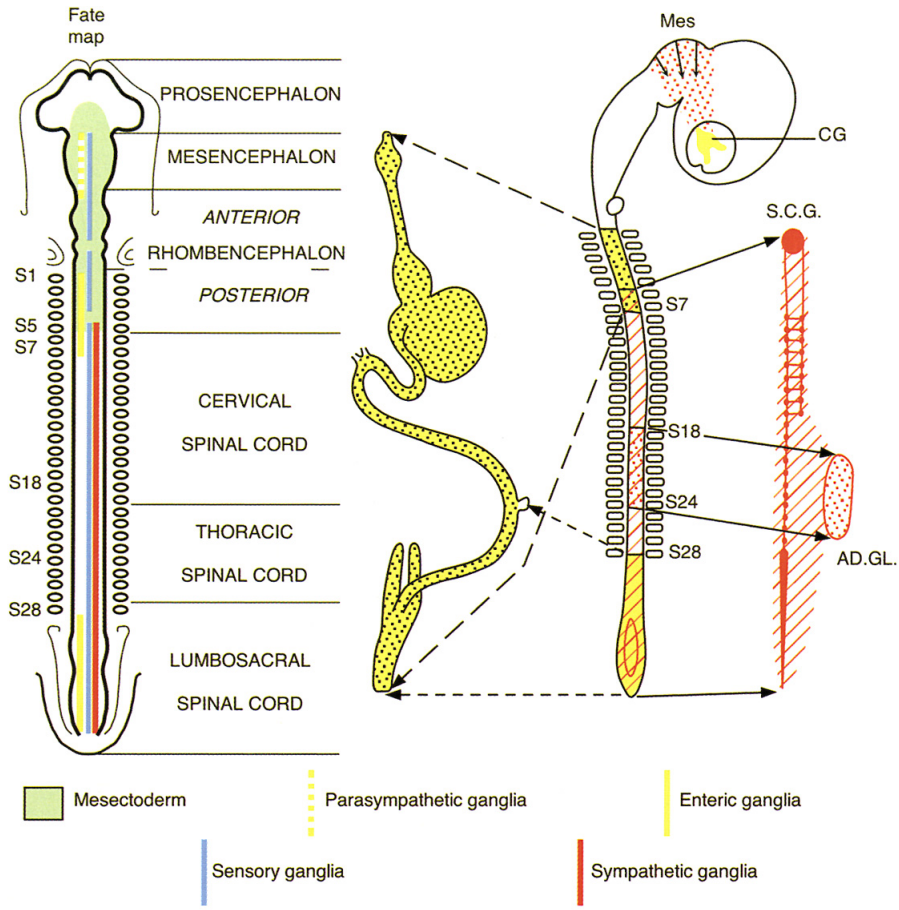

Figure 5.1 The origin of autonomic ganglia, enteric ganglia, and adrenomedullary cells. The neural crest caudal to the level of the fifth somite pair gives rise to the ganglia of the sympathetic chain. The adrenomedullary cells originate from the neural crest between somite levels 18 and 24. The vagal neural crest (somites 1–7) gives rise to the enteric ganglia of the preumbilical region, the ganglia of the postumbilical region originating from both the vagal and the lumbosacral neural crest (see text for further details regarding mammals; see also Fig. 5.9). The ganglion of Remak (RG) is derived from the lumbosacral neural crest (posterior to level of somite 28). The ciliary ganglion (CG) is derived from the mesencephalic crest (Mes). AD.GL., adrenal gland; S.C.G., superior cervical ganglion.

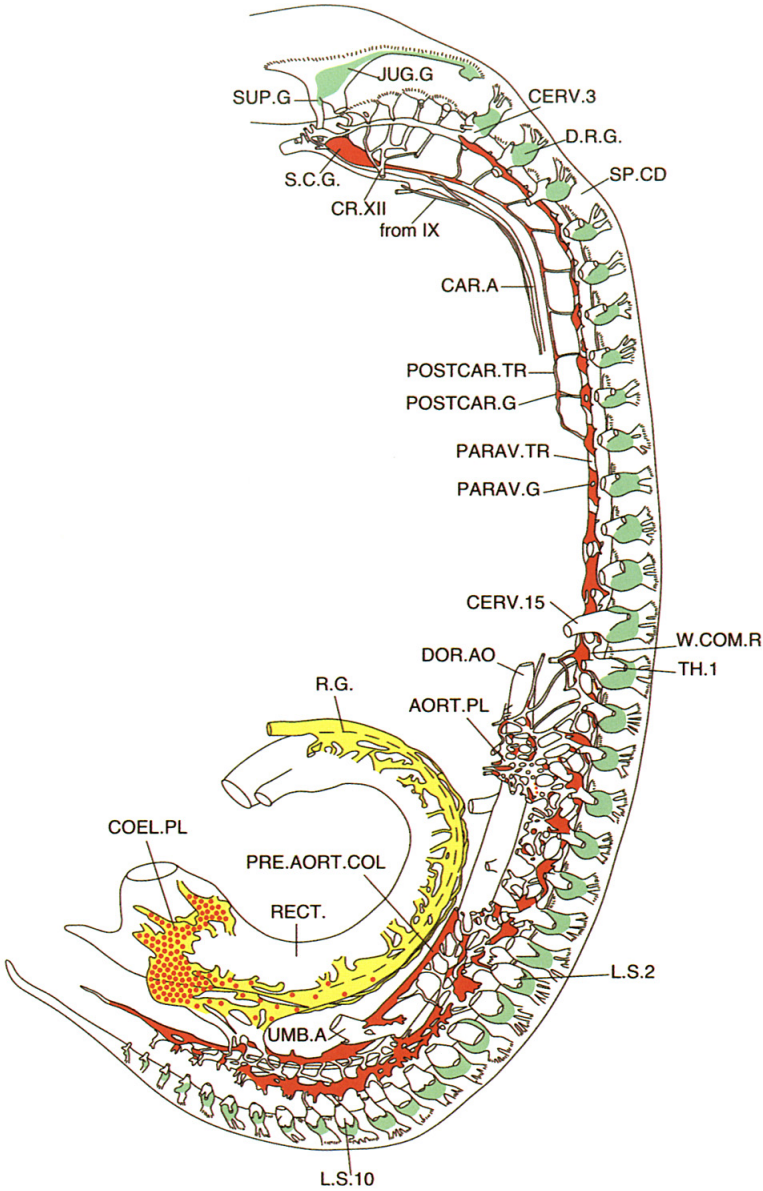

Figure 5.2 The organization of the peripheral ganglia and plexuses of the 8-day-old chick embryo. AORT.PL, aortic plexus; CAR.A, carotid artery; CERV.3, cervical nerve 3; CERV.15, cervical nerve 15; COEL.PL, coeliac plexus; CR.XII (from IX), cranial nerve; DOR.AO, dorsal aorta; D.R.G., dorsal root ganglion; R.G., Remak ganglion; JUG.G, jugular ganglion; L.S.2, lumbosacral nerve 2; L.S.10, lumbosacral nerve 10; PARAV.G, paravertebral ganglion; PARAV.TR, paravertebral trunk; POSTCAR.G, postcarotid ganglion; POSTCAR.TR, postcarotid trunk; PRE.AORT.COL, preaortic column; RECT., rectum; S.C.G., superior cervical ganglion; SP.CD, spinal cord; SUP.G, superior ganglion; TH.1, thoracic nerve 1; UMB.A, umbilical artery; W.COM.R, white communicating ramus. (Modified from Yntema and Hammond, 1945, and Hammond and Yntema, 1947.)

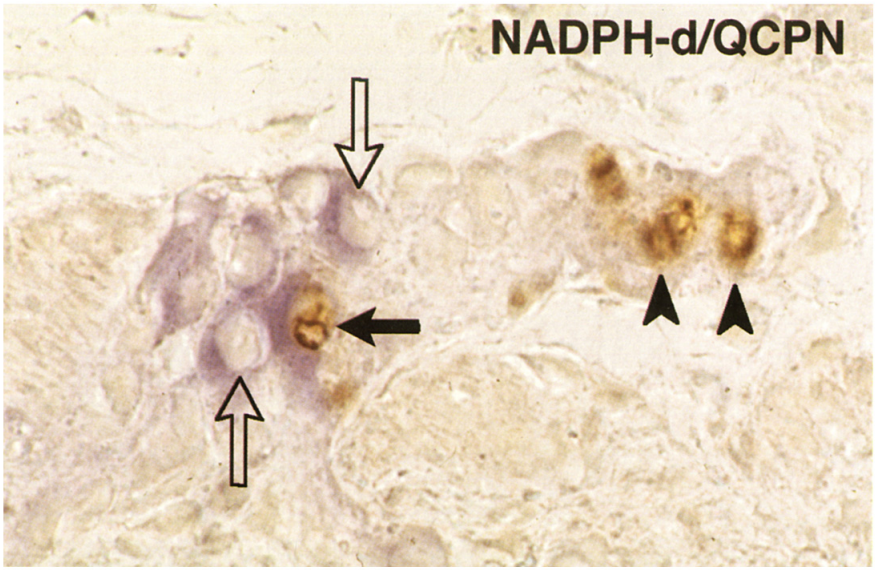

Figure 5.4 The sacral-level neural crest contributes to intestinal neurons. NADPH-diaphorase histochemistry. Myenteric ganglion. NADPH-diaphorase stained the cytoplasm of neurons violet (open arrows), while the nuclei of quail cells were stained brown (arrowheads). Double-labeled neurons possessed violet cytoplasm with brown nuclei (arrow). (Reproduced, with permission of Company of Biologists Ltd, from Burns and Le Douarin, 1998.)

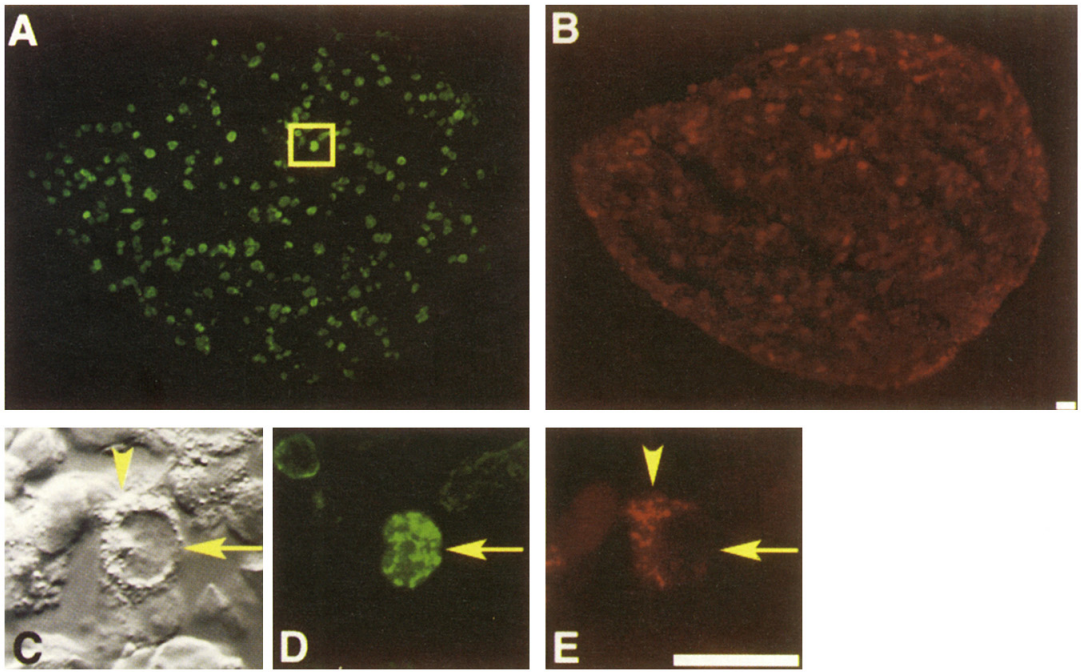

Figure 5.6 Mitotically active superior cervical ganglion (SCG) neuroblasts possess axons projecting into efferent nerves. To identify dividing neuroblasts bearing axonal projections *in vivo*, E16.5 rat embryos were labeled with bromodeoxyuridine (BrdU) for 1 hour and fixed afterwards. BrdU labeling was combined with retrograde rhodamine dextran tracing as follows: SCG was dissected, the efferent internal and external carotid nerves were sectioned with dextran-coated knives 1 mm from the ganglion, and the explant was incubated for 4 hours in culture to allow retrograde transport. Confocal images of 8-μm sections indicate BrdU nuclear labeling in A and dextran labeling in B. Higher magnification of the boxed region in A illustrates a neuroblast in C by DIC optics that colocalizes nuclear BrdU (arrow, D) and retrograde cytoplasmic tracer (arrowhead, E). Bar = 25 μm. (Kindly provided by E. DiCicco-Bloom.)

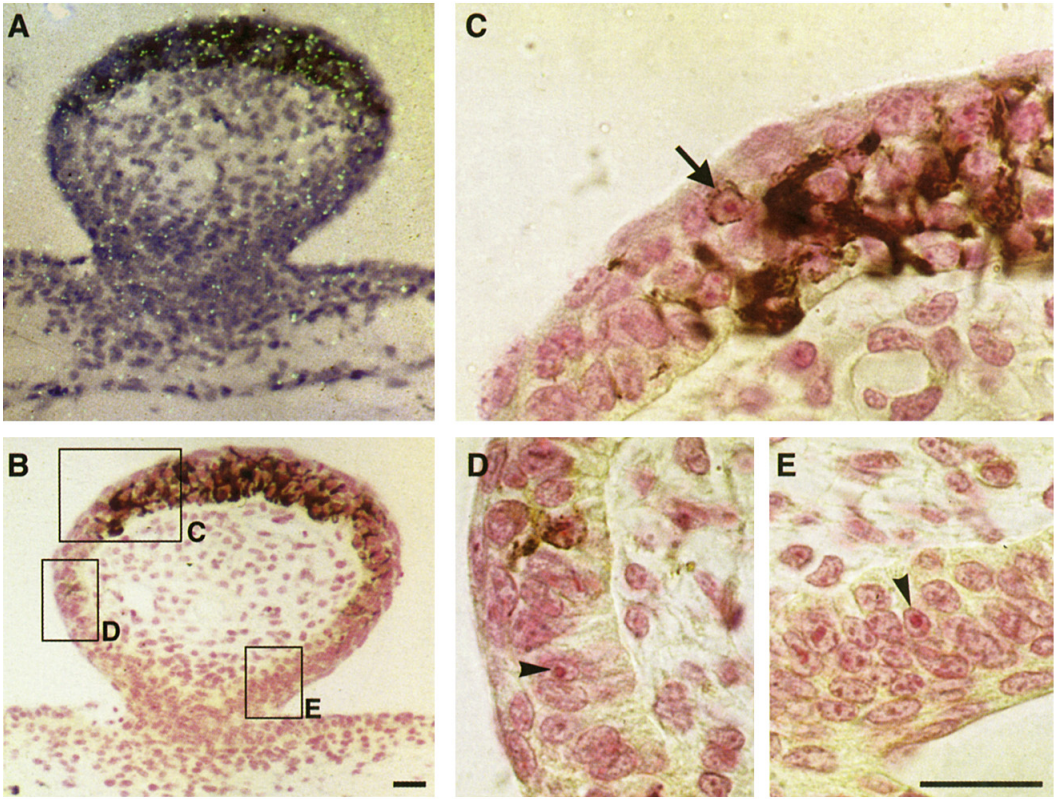

Figure 6.8 *Sl* expression associated with Feulgen–Rossenbeck staining showing quail cells of neural crest origin in a quail–chick chimera. *Sl* expression in a feather bud of a quail–chick chimera at the beginning of melanogenesis. A quail neural tube was grafted in a 15ss embryo isotopically and isochronically at level of somites 8–14. Fixation was performed at E11 (HH 37). (A) *In situ* hybridization with a radioactive *Sl* riboprobe on a feather bud of the dorsal pteryla. *Sl* is mainly expressed in the epidermis of the top of the bud and is no longer expressed in the rest of the skin epidermis. (B) Adjacent sections were subjected to Feulgen–Rossenbeck staining. The framed areas are enlarged in C, D, E. At the top of the feather bud, quail cells are pigmented (arrow in C), whereas quail cells at the basis of the feather bud are still undifferentiated (arrowheads). Bar = 17 μm. (Reproduced, with permission, from Lecoin *et al.*, 1995.)

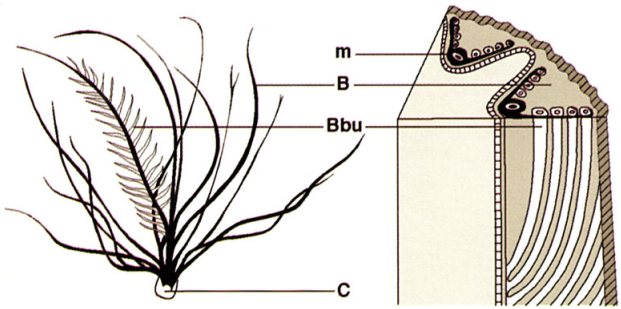

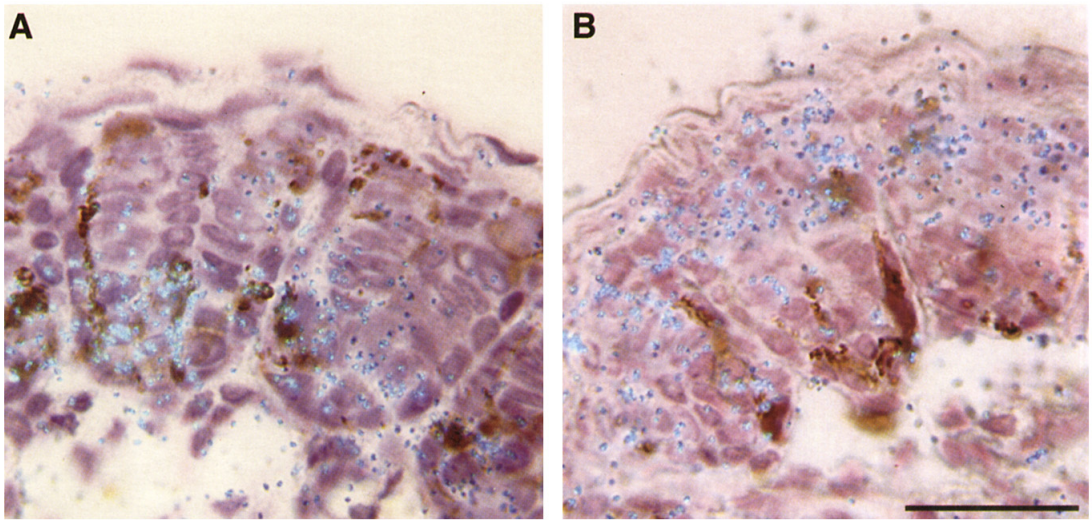

Figure 6.9 Top: Schematic drawing of a down feather modified from Watterson (1942). The melanocytes (m) are located at the inner side of the barb ridge (B) and deliver their pigment granules to the outermost barbule cells (Bbu). C, calamus. Bottom: Complementary expression pattern of *c-kit* and *Sl* in the developing feather. *In situ* hybridization with *c-kit* and *Sl* radioactive riboprobes on E13 feathers sectioned transversally. (A) Melanocytes expressing the *c-kit* gene are located at the basis of the barb ridge, whereas *Sl* is expressed by the barbule cells at the periphery of the feather (B). It is therefore conceivable that the Steel factor attracts the melanocyte processes towards the outermost aspect of the barb while they deliver pigment to the barbule cells. Thus, the c-kit/Steel system is likely to play a role in the transfer of the melanosomes from the melanocyte to the keratinocyte. Bar = 26 μm. (Reproduced, with permission, from Lecoin *et al.*, 1995.)

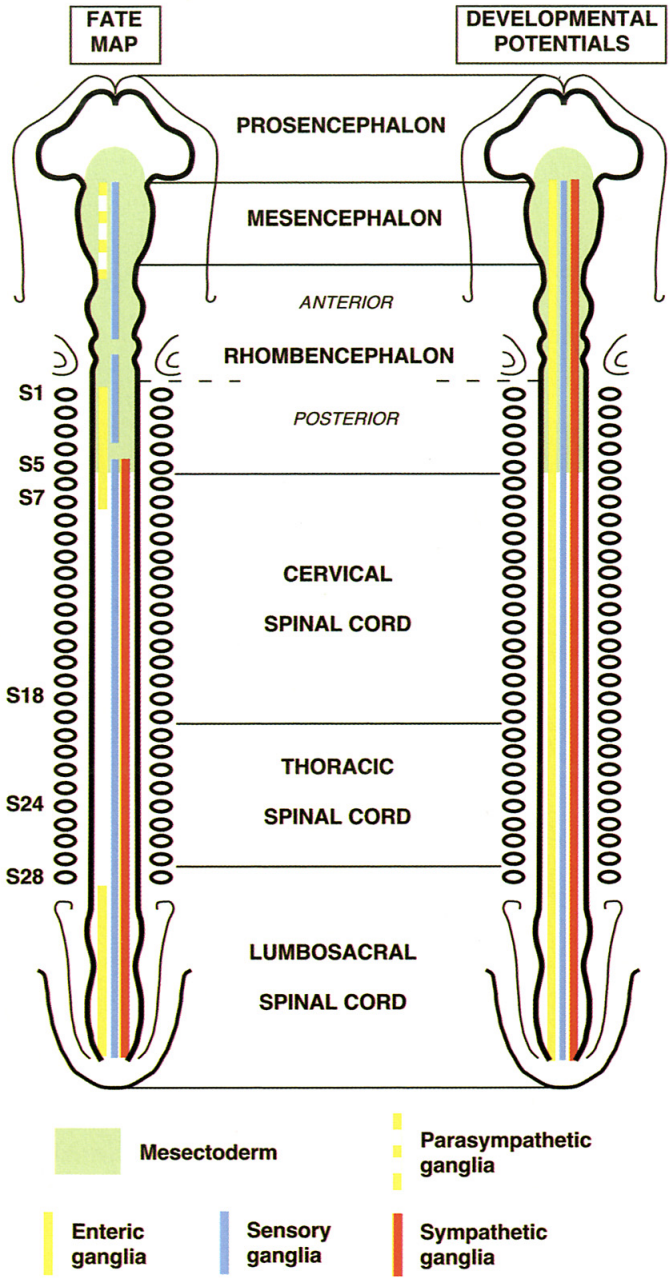

Figure 7.1 Fate map and development potentials of the neural crest along the axis. Left: Fate map of the presumptive territories along the neural crest yielding the mesectoderm, the sensory, sympathetic and parasympathetic ganglia in normal development. Right: Development potentials for the same cell types as shown in the fate map are indicated. Results are based on isotopic and heterotopic grafting of neural primordia between quail and chick embryos. See text for details. (Reprinted, with permission, from Le Douarin, 1986. Copyright (1986) American Association for the Advancement of Science.)

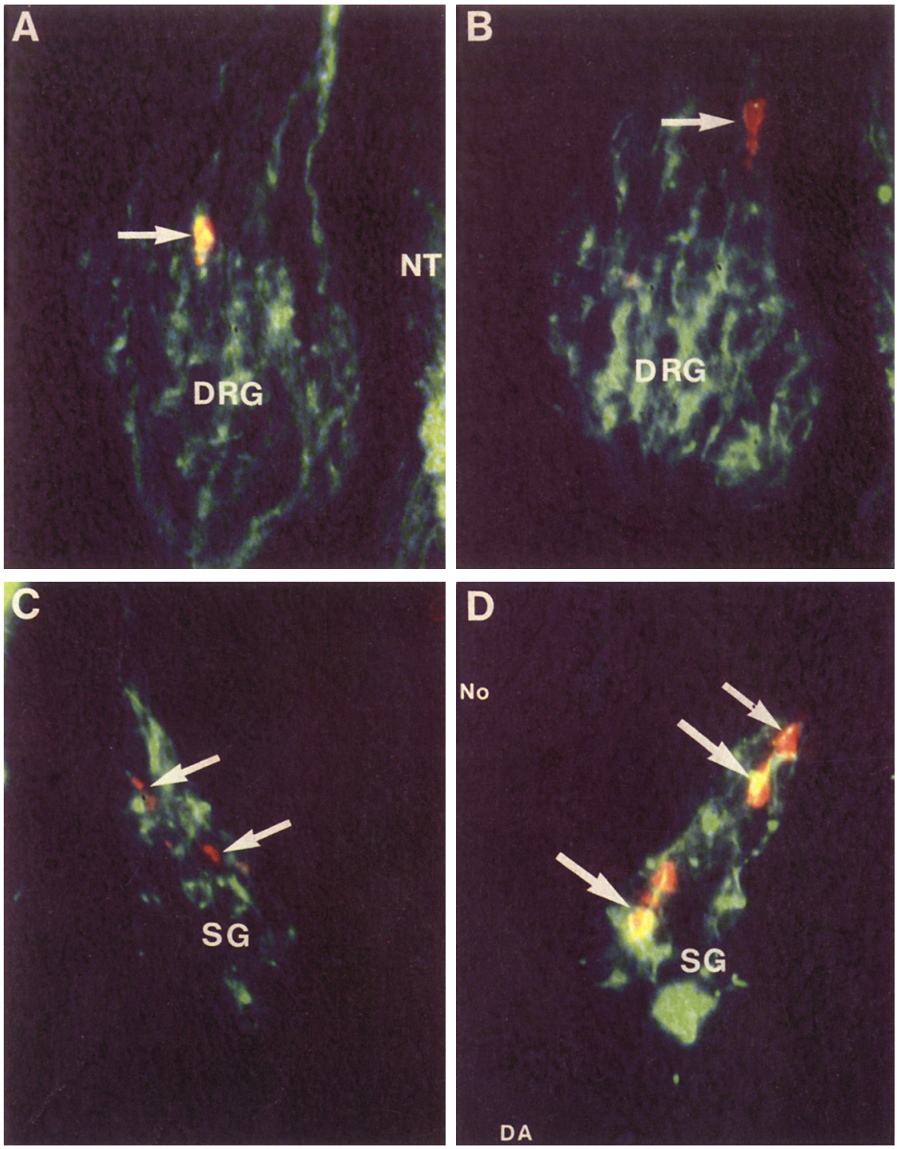

Figure 7.4 Lineage analysis of trunk neural crest. Neurofilament expression in lysinated rhodamine dextran (LRD)-labeled descendants. LRD labeling is shown in red, and staining with an antibody against neurofilament (NF) protein is shown in green. (A–C) Images from an embryo that contained LRD-labeled cells in the DRG, sympathetic ganglion (SG), and ventral root (VR, not shown). (A) An LRD-labeled cell (arrow) in the DRG has bright NF staining in its axon. Orange color indicates double NF/LRD staining. (B) Another cell in the DRG is NF− and has the appearance of a support cell. (C) The SG of the same embryo showing two NF− cells. (D) The SG of another embryo contains numerous cells (arrows) with large cell bodies and NF+ axons. (See Fraser and Bronner-Fraser, 1991, for details; reproduced with permission of Company of Biologists Ltd.)